ULTRA-SENSITIVE DETECTION OF HCG

USING

A MICRO-RESONATOR BASED BIOSENSOR

By

Zhikun Wang

_____

A Report Submitted to the Faculty of the

COLLEGE OF OPTICAL SCIENCES

In Partial Fulfillment of the Requirements
For the Degree of

MASTER OF SCIENCE

In the Graduate College

THE UNIVERSITY OF ARIZONA

2019

STATEMENT BY AUTHOR

This thesis has been submitted in partial fulfillment of requirements for an advanced degree at the University of Arizona and is deposited in the University Library to be made available to borrowers under rules of the Library.

Brief quotations from this thesis are allowable without special permission, provided that an accurate acknowledgement of the source is made. Requests for permission for extended quotation from or reproduction of this manuscript in whole or in part may be granted by the head of the major department or the Dean of the Graduate College when in his or her judgment the proposed use of the material is in the interests of scholarship. In all other instances, however, permission must be obtained from the author.

SIGNED:

APPROVAL BY THESIS DIRECTOR

This thesis has been approved on the date shown below:

_____ _____

Tsu-Te Judith Su Date

Assistant Professor of Optical Sciences

ACKNOWLEDGEMENTS

I would like to thank my family to give me consistent support.

I would like to thank Professor. Su for her beneficial advice during the whole experiment procedure and her help in writing report. Your advice in doing experiments and learning new knowledge inspired me to go further into the optics. You really give me a new perspective of exploring the world of Photonics.

I would like to thank every member of Little Sensor Lab for their generous help during the experiment. I especially want to thank Dr. Ozgur, thank you for your teaching and participating. From theory to hands-on experiments, I have learned numerous technical skills from you.

I would like to thank my committee, Professor. Tsu-Te Judith Su, Professor Masud Mansuripur, Professor. Dae Wook Kim. I am so impressed by their enthusiasm and patience in helping students. Their knowledge and kindness motivate me to keep learning and become better.

Thanks for other teachers and staffs in OSC! Thank you for your help in the past two years. It really gives me an excellent experience of studying in OSC unforgettable!

Table of Contents

List of Figures 5

Abstract 6

1. Introduction 7

1.1 Basic concept of WGM (Whisper Gallery Mode) Microresonators 7

1.2 Method for biodetection (FLOWER system) 10

2. Fabrication of microcavity & Optical coupling 14

2.1 Microcavity fabrication 14

2.2 Fiber tapering & coupling 17

3. Experimental Setups 21

4. Thermal Effect in Microcavity 25

5. Experiments about hCG detection 28

5.1 Microtoroid functionalization 28

5.2 Liquid preparation and infusion 29

5.3 Data recording 29

6. Data Analysis 31

7. Results 33

8. Summary 37

9. Reference 38

List of Figures

Fig.1 a) Schematic of Microtoroid b) Schematic of Microsphere 9
Fig.2 Mode distribution in Microcavity (Microring, fundamental mode).....9
Fig.3 Mode distribution in Microtoroid (cross section).....10
Fig.4 Schematic of FLOWER system.....12
Fig.5 Transmission diagram from computer.....13
Fig.6 Operation window of frequency locking system.....13
Fig.7 Microtoroid before reflowing 16
Fig.8 Microtoroid after reflowing 16
Fig.9 Microsphere 17
Fig.10 Micro-aquarium for liquid infusion & detection.....24
Fig.11 Relationship between temperature & WL shift.....26
Fig.12 Thermal effect related experimental setup 27
Fig.13 Schematic for surface chemical combination [18].....30
Fig.14 Schematic for infusion.....30
Fig.15 Data analysis through Matlab.....32
Fig.16 Result of hCG detection from a simulated sample.....35
Fig.17 Result of hCG detection from real sample 36
Fig.18 comparison of FLOWER and other sensing methods.....37

Abstract

Recently, it's harder for clean sports competition nowadays since drugs production technology increases faster than the optimization of sensors. Moreover, microcavities have attracted more interests as a sensor due to its variety of advantages such as ultra-sensitive and real-time measurement. There is a strong demand for the high-sensitive and convenient sensor that can be utilized for drug detection. Here we show a new type sensor with ultra-high sensitivity. The following presents the basic concepts of micro-resonator, the thermal effect inside the micro-resonator, and a new type sensor based on "frequency-locked microtoroid optical resonators" for human chorionic gonadotropin (hCG)detection. For the microtoroid we are using, with the temperature changes 1 degree in Celsius, there is a 5 pm resonance wavelength change. By using this new method for detection, it gives us three orders of magnitude of improvement in the limitation over mass spectrometry, the gold standard for hCG detection nowadays. We anticipate our result as a starting point for ultra-high sensitive detection, which may a possible solution for clean sports competition and early diagnosis.

1. Introduction

1.1 Basic concept of WGM (Whisper Gallery Mode) Microresonators

Basically, the whisper gallery mode microresonator is a resonator, as its name indicated. When light transmitted into it, it will be “trapped” by the resonator because of the TIR (totally internal reflection). However, only the light which its wavelength equals to the optical perimeter over an integer can become stable since every time the light travels through the microresonator (for example, a microsphere) for a circle, the phase is equal to the phase it starts the travel. Then constructive interference was created, and resonance happened. The resonance wavelength related to the optical perimeter, and the optical perimeter related to the effective refractive index of the mode of travel light. This parameter will change with the size of microresonator changes or the ambient environment refractive index change. Based on that phenomenon, we can use the microresonator as a detector. If the resonance wavelength has a blue or redshift, it means that there’s an ambient environment of microresonator’s refractive index change, which may due to the biomedical combination or material concentration changes. Then the result can be received through the wavelength changes & data analysis.

Then let’s talk about modes in the microcavity. In my point of view, modes can be described as the route that light travels in the waveguide. Start with the basic waveguide modal, a silicon rod with infinity length exposures in the air. The refractive index of the silica rod is 1.5 while the refractive index is 1. Now if we know the radius of the silica rod, then the number of radial modes in the waveguide (silica) and distribution of each mode can be calculated by using the Helmholtz equation:

$$(\nabla^2 + k^2)\mathrm{A} = 0$$

Though it's a little bit difficult to calculate it through hands-on calculation, it's easy to solve this problem if we use Matlab to solve it in Matrix. Now back to our microcavity, just imagine that the silica rod was bent, and its head connects to its tail, then we get a structure in microcavity field called microring. The only difference between silica microring and silica rod is microring is bending, so if we find a way mapping each point on the silica rod to the silica microring, then we can also solve the mode number and distribution by solving the Helmholtz equation!

Luckily, there are one method called conformal mapping [1], which investigated at 2002, can help us to finish this part. When do the conformal mapping, the changed parameter is the refractive index in Matrix:

$$n' = n^{u/R_2}$$

Where:

$$\mathrm{u} = -R_2 \ln(R_2/R_1)$$

In these two equations, n prime is the refractive index after conformal mapping while n is the RI before mapping, u is a parameter to simplify the calculation, R_2 is the outer radius of the microring, R_1 is the inner radius of the microring. After the conformal mapping, we can get the mode information of microring by solving the Helmholtz equation. Moreover, COMSOL can also be used to solve the mode related question through its electromagnetic waves, frequency domain method. This software has the wave equation inside itself and can help us to calculate the correct answer by FEM (finite element method). [2]

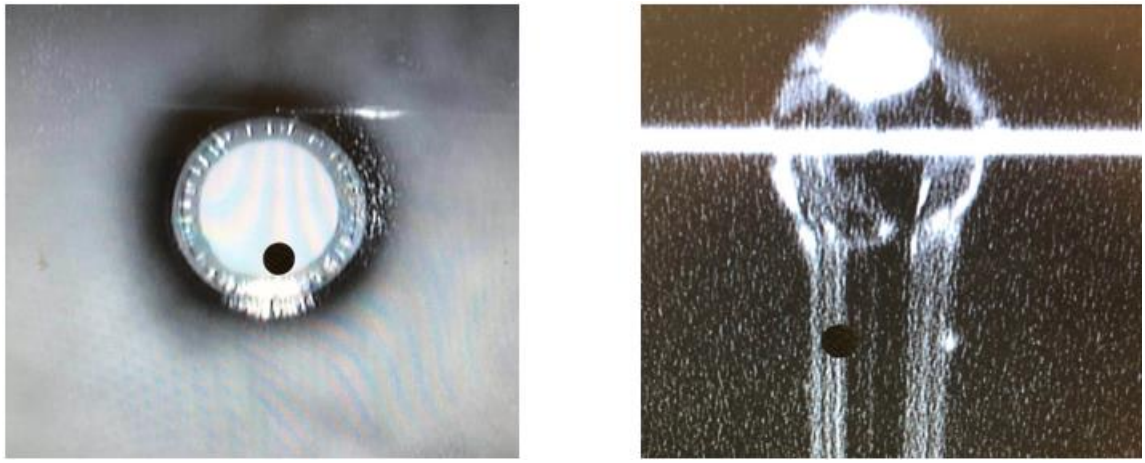

Fig.1 a) Schematic of Microtoroid b) Schematic of Microsphere

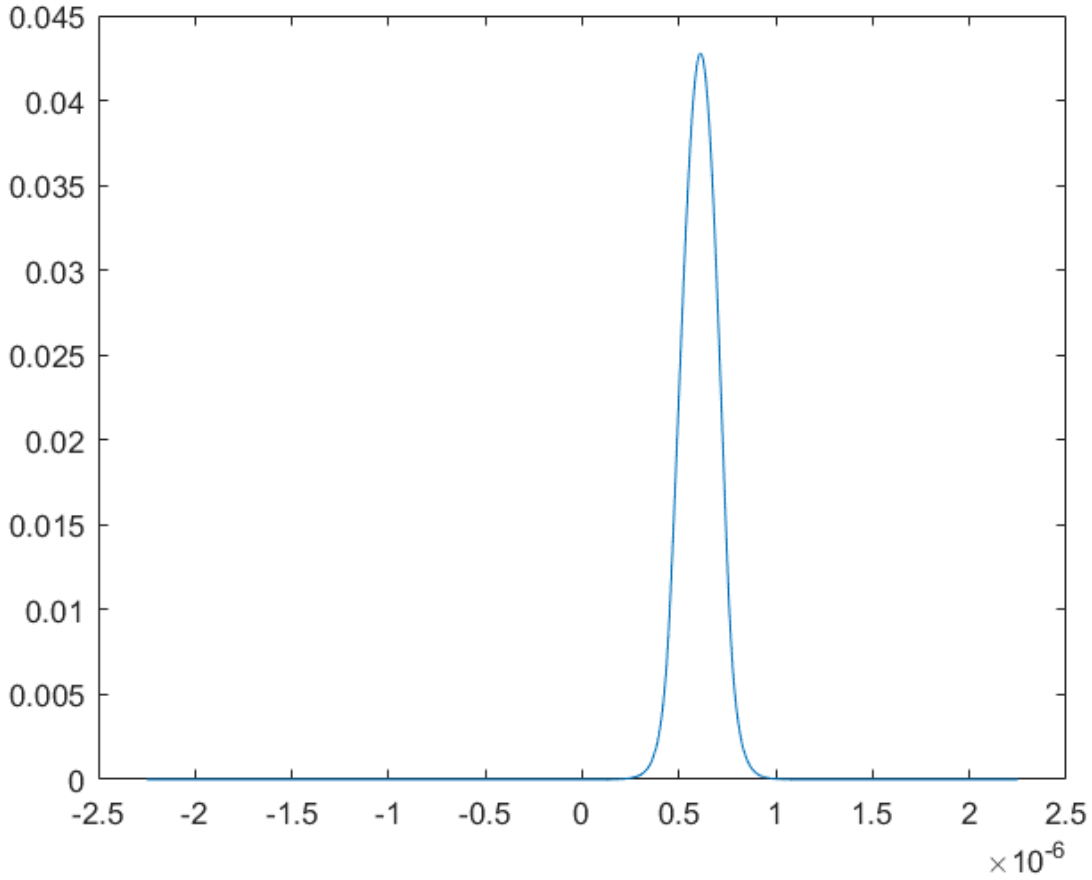

Fig.2 Mode distribution in Microcavity (Microring, fundamental mode)

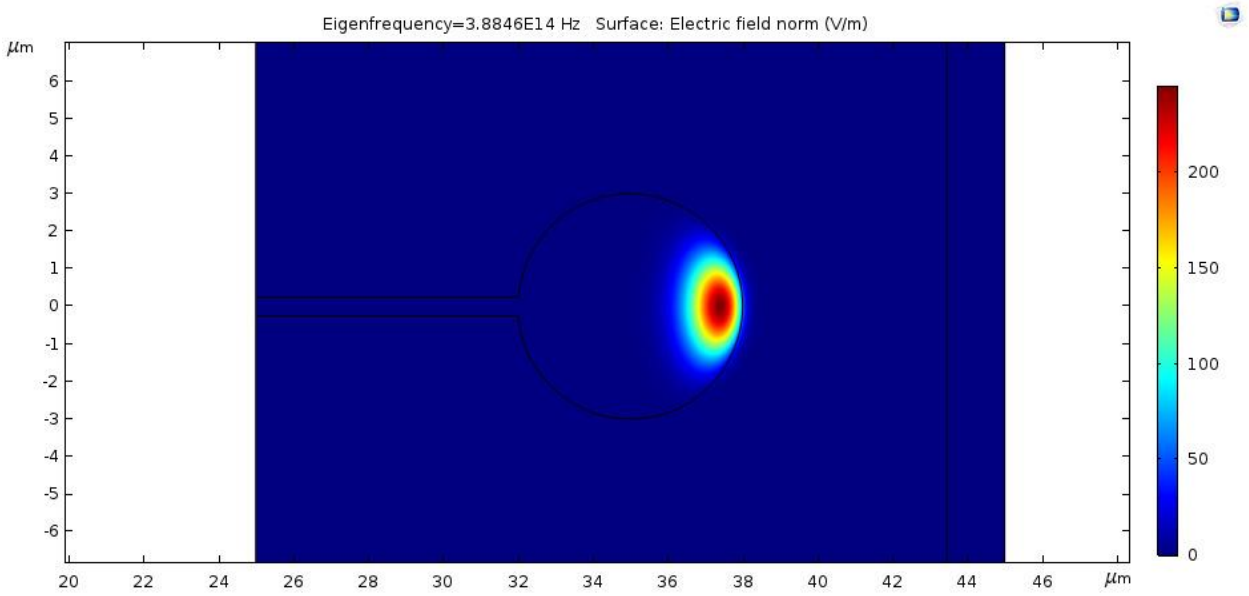

Fig.3 Mode distribution in Microtoroid (cross section)

1.2 Method for biodetection (FLOWER system)

This part I will introduce the working concept of FLOWER system that I used for this detection. The full name of FLOWER system is “frequency locking optical whispering evanescent resonator”. It uses microcavity as a detector, mapping the refractive index changes by tracking the resonance wavelength shift, thus show up the characteristics of microcavity’s ambient environment. While most types of the microcavity-based resonator are relied on finding the resonance by continuously sweeping the tunable laser to locate the resonance frequency, the FLOWER system tracks the resonance by locking the laser output wavelength directly equal to the resonance of the microcavity. Compared with other methods, this method can decrease the noise and increase the sampling frequency since while other methods get resonance by sweeping the whole spectrum, FLOWER system will only give laser a voltage modulation to modulate its output wavelength equal to the resonance wavelength. So basically, once we have the initial output wavelength without voltage modulation, there is a mapping between the amplitude of voltage

for modulation and the position of resonance wavelength, thus we can get the resonance data rapidly without anything related to transmission spectrum.

Fig. 4 is the schematic diagram for the FLOWER system. To simplify the procedure of how FLOWER system works, I would like to divide the whole system into four parts: data acquisition module, locking module, detection module, and light source module. Let's begin on the light source part. At first, we use the computer to drive the 780nm laser light source, which can emit a continuous laser beam around 780nm with output power about 1mW. Then light travels into a scroll of fiber and goes through a 3dB optical coupler that can divide light into to part with power ratio 1:1. After the optical coupler, one branch of light gets into the tapered part, generating the evanescent field around tapered fiber and transmit the signal to the auto-balanced photodetector. The other branch of light just goes into the auto-balanced photodetector directly as a reference to remove the noise to remove the error from the original laser beam source. Now we can get data from auto-balanced photodetector that includes the output intensity of the signal arm after the auto balance effect in a certain wavelength (frequency). In this situation, we didn't do the locking step, but just input a continuous voltage with frequency equals to 100 Hz to modulate the center wavelength of laser beam source. So, after that, we can get a diagram through the computer that shows the relationship between output intensity and wavelength. Currently, what we've gained from the computer is the transmission diagram of the light travel through the microcavity. If we find a dip in the transmission diagram, which means the resonance frequency founded, then we can do the frequency locking by using the Digilock 110 from Toptica Photonics. Technically, the locking procedure was achieved by applying a 2kHz sine dither signal to generate an error signal for locking. PID (proportional-integral-derivative) controller also be applied in this step to track the changes in the

resonance frequency. When the locking system successfully tracking the resonance frequency of the microcavity, instead of a continuously 100Hz voltage modulation, it will enable a voltage output to modulate the center frequency of output laser beam so that the center wavelength of the light source will be fixed with the resonance wavelength. Meanwhile, this voltage output will also be recorded to the computer through a data acquisition card. Since we know the initial center wavelength of the light source and the ratio between the modulation voltage and center wavelength shift from voltage modulation, thus we can figure out the resonance frequency of the microcavity in real-time.

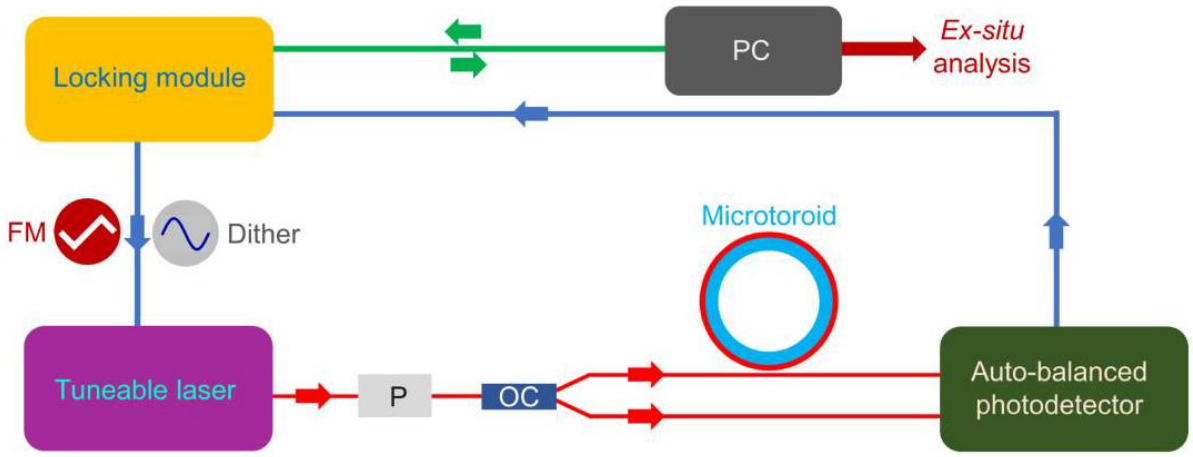

Fig.4 Schematic of FLOWER system

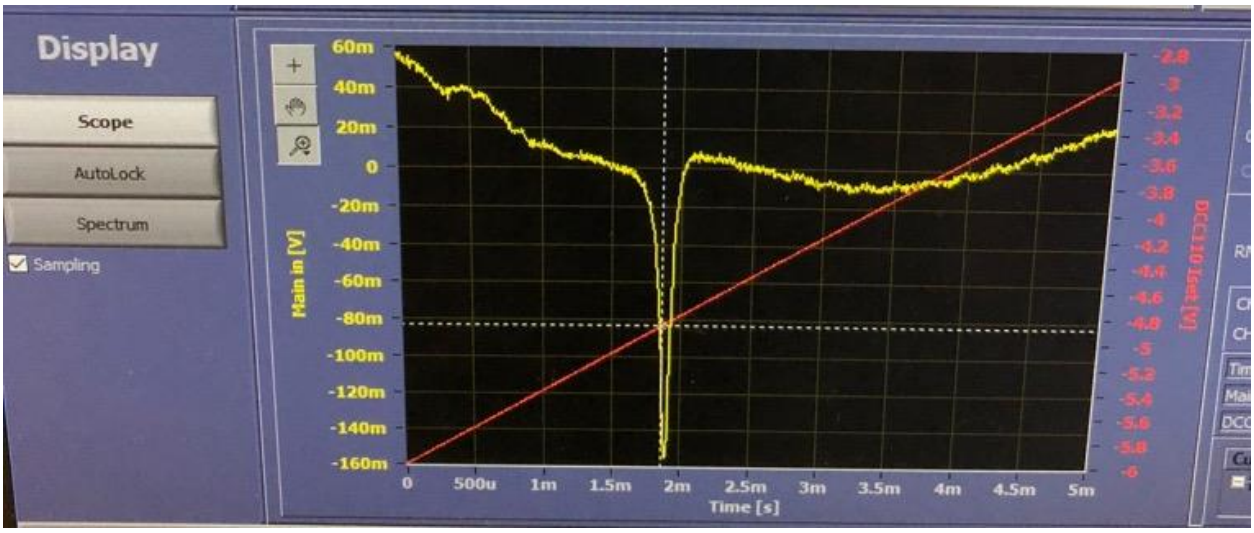

Fig.5 Transmission diagram from computer

Fig.6 Operation window of frequency locking system

2. Fabrication of microcavity (microsphere and microtoroid) & Optical coupling

2.1 Microcavity fabrication

In this research, microcavity can be specialized as microcavity and microtoroid. This part will introduce the fabrication steps of microtoroid and microsphere.

First, let's talk about microtoroid. Since we build the microtoroid array via silica, it's easy for us to start the fabrication with the silicon chip. For microcavity fabrication, we use a ~ 6 mm x 4 mm silicon chip as the substrate of our microtoroid array. The fabrication of microtoroid array begins with some oxidation reaction, which can convert one surface of the silicon chip to silica. The thickness of the silica surface is about 2 microns. Then the silica surface of the chip was cleaned up and coated with a layer of photoresist for lithography. After the photoresist coated on the surface, the chip will be overlapped with a mask that has the array pattern and then exposed on UV light for lithography procedure. Now there should have a silica array on the silicon chip. Next step for microtoroid fabrication is washing and etching. Before the etching step, the chip should be washed with acetone to remove the photoresist layer on the silicon surface. Now the silicon chip only contains a silica array on its surface without any other components and will be stored in vacuum for protection. After that is the etching step. For etching, a Xactix xenon difluoride etcher is used. XeF_2, the chemical reagent that will be utilized for etching, has numerous advantages. First, it has high selectivity in etching procedure for SiO_2/Si structure that will only etch Si but not harm SiO_2 surface. [3] Second, when we use XeF_2 for etching, it will produce a fluoro silyl layer, which can block conjunction between silicon and O_2 plasma so that hydroxyl will not be combined to silicon substrate if we use hydroxyl for biomarker conjugation.[4] When etching step finished, we will have a silicon chip

substrate covered with some array structure looks like “mushroom”. These mushrooms have its head in silica and its body in silicon. This type of “mushroom” can be called as microdisk since the silica part looks like a disk. However, due to the thin thickness and boundary edge of the disk, it has small a mode area for detection. So, the silica disk will be reflowed by CO_2 laser then convert the disk structure into toroid structure, which has a bigger mode area than disk. To finish the reflowing step, a CO_2 laser at 10.6 microns of its center wavelength will be used for reflowing. First the CO_2 will be aligned to the center of microdisk structure with a HeNe laser’s help as a reference laser (since CO_2 laser is invisible), then the laser was turned on and controlled by a function generator’s output signal because microdisks are very small and it only needs a little bit energy to heats up the structure, otherwise it will be overflowed and crack will be found on microtoroid’s surface. The reason why we use CO_2 laser with 10.6 micron of its center wavelength is that silica has high absorption for 10.6 microns CO_2. So, when laser heats up the center of silica microdisk, the temperature of silica structure will increase to a very high number and then silica will be melted and reformatted as a microtoroid with an extremely smooth surface. The whole procedure of reflowing will be monitored through a digital microscope.

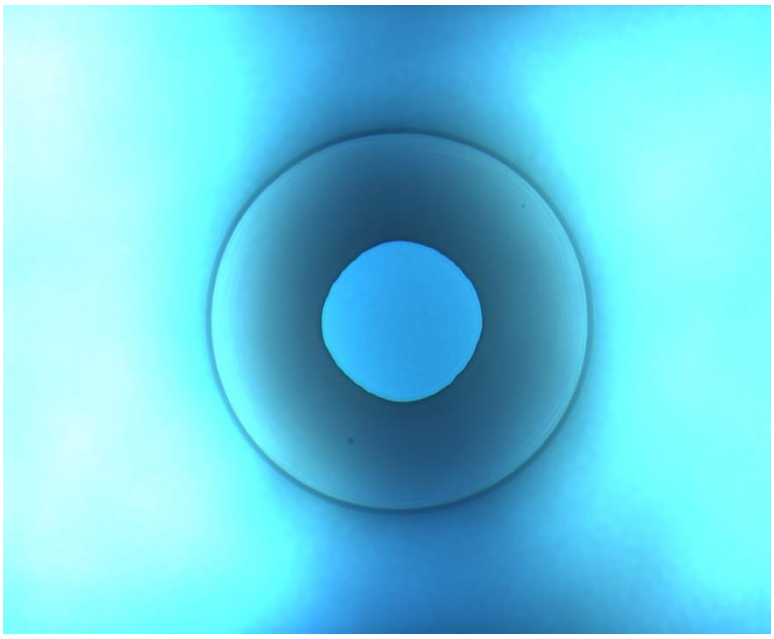

Fig.7 Microtoroid before reflowing

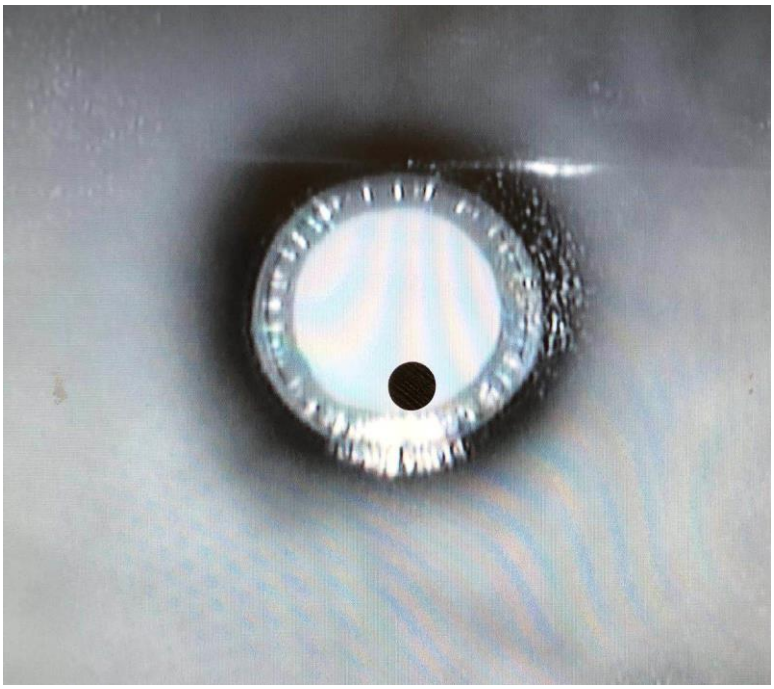

Fig.8 Microtoroid after reflowing

Compared with microtoroid, microsphere is much easier to be fabricated. First, we choose a cut of single mode fiber, then use the wire stripper to remove the buffer &

jacket so only core and cladding remain. After that fiber cutter will be used to cut one end of this fiber so that the cross section of that cutting end will be very smooth. Next, the fiber end with a smooth surface will be located at the same position as the silicon chip with some microdisk located at the reflowing system for reflowing. Since the diameter of the fiber is larger than the microdisk and we expected to get a sphere, which means the volume of itself is hugger than microtoroid, the laser output will be the continuously pump laser instead of the pulse laser. To make a microsphere, the smooth end of fiber should overlap with the lower boundary of the monitor and center of the monitor should overlap with fiber. Then turn the laser on with power indicator shows 7.5%. Since silica has high absorption for CO_2 laser with its center wavelength close to 10.6 microns, the fiber on the monitor will be melted quickly and then shrink to a sphere. Keep the laser heat up for 20 seconds then turn the laser off and we get the smooth microsphere for the experiment.

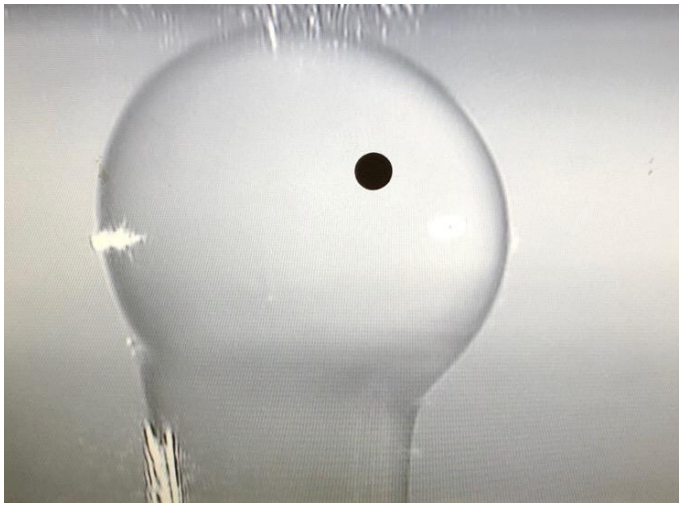

Fig.9 Microsphere

2.2 Fiber tapering & coupling

Now we have a microcavity that can help us for detection. But how can we insert energy into the microcavity? Basically, the easiest way to achieve our goal in to

use a coherent light source to illuminate the microcavity and wish to see the resonance through scattering. However, direct light-microcavity coupling is very inefficient. [5] To coupling energy into the microcavity, it's more effective to use evanescent wave for coupling instead of normal light. There are several ways to reach the goal. The first method being mention through the reference is a paper published in 1989. [6] In this paper, the author tried to use a high-index prism with TIR (totally internal reflection) to achieve the goal. Since the evanescent wave for coupling always comes from TIR, then optical fiber attracts the researcher's eye. There is another type of coupling method mentioned in 1999. This coupling method uses an angle-polished optical fiber tip for coupling and the efficiency of it is about 60%. [7] However, the method that widely used for evanescent wave coupling nowadays are using a tapered fiber for coupling, which proposed in 1998 [8] and optimized by Vahala group [9]. The coupling efficiency of this method can be up to 99.8%. So, the method of using tapered fiber for evanescent wave coupling has been chosen for this experiment.

To finish the fiber tapering, the machine from Newport to stretch the fiber and hydrogen flame will be used. First, we use the stripper to remove a sag of jacket & buffer that close to the end of optic fiber. The length of this sag should be around 2cm. After that acetone will be used to clean up the region without buffer & jacket and then put this region to the machine. Next, we change the position of hydrogen flame's position and height to make sure that the tip of hydrogen flame is used for heating up procedure. Then the fiber without jacket & buffer will be held by two fiber clamps and slide along two steel rods. With the stretching of two fiber clamps and the hydrogen torch heats-up effect, the fiber is first softened and then stretches to longer length with lower diameter. Details of fiber tapering can be seen on reference [10]. Although we have a microscope to monitor the diameter of the

tapered part during the tapering, it's still very hard to figure out the time of stop tapering only through a microscope. Actually, after tapering starts several minutes, we can see the light transmitted from laser to the end of fiber oscillates. This oscillation is due to the interference between different modes and its frequency increases with time. The most important feature for a good tapered fiber is to see the intensity of fluctuation decreases, which means the tapered fiber goes from tapered multimode to tapered single-mode [10]. In this situation, the diameter of tapered fiber waist is in units of wavelength and it can be used for our experiment for optical coupling.

Now we have microcavity for detection and tapered fiber for light coupling. As mentioned before, the tapered fiber waist will be used to emit the evanescent field and then coupling light into the microcavity. When light transmitted through the tapered region, the waveguide structure is totally different from the normal optic fiber. Light transmitted through the fiber based on TIR. For example, single-mode fiber transmitted the light inside through its core. When light travels to the boundary between core and cladding, there is a TIR happened due to Maxwell's equation. So, the light will be confined in the core region and we can detect evanescent field in the cladding region for fundamental single mode fiber. However, in this experiment, the boundary between cladding and core in the tapered part is annihilated due to the hydrogen flame's heat up effect. Then the waveguide structure turns from cladding-core-cladding to air-tapered part-air and evanescent field is exposed in the air. This evanescent field can be utilized as a source to illuminate microcavity. Moreover, the coupling between microcavity and tapered fiber is in both way: light coupled from tapered fiber to microcavity and light coupled from microcavity back to tapered fiber. For both coupling phenomenon, there is a $\pi/2$ phase shift. So, compared with the light in the tapered

fiber, the light coupling back from microcavity will induce a π shift in phase. If the light wavelength and the radius of microcavity fit with the following equation:

$$m\lambda = 2\pi r n_{eff}$$

m means the mode number, while lambda means the light wavelength and r means the radius of the microcavity, n_{eff} means the effective refractive index of that mode. Thus, there is a destructive interference happened. This destructive interference will give us a dip through the transmission spectrum. We will detect that dip changes through our FLOWER system and use it as a parameter for detection.

3. Experimental Setups

This chapter I will introduce the basic procedures of an experiment related to FLOWER system. The whole experimental procedure can be separate into three parts: experiment material preparation, finding the resonance frequency with high Q factor, infusion of liquid to be tested and data recording.

To begin with the experiment about using FLOWER system for detection, the first thing is to produce a sag of tapered fiber and microcavity. Compared with microsphere, since microtoroid has higher Q factor [11], we always use microtoroid for experiment instead of the microsphere. Steps of making tapered fiber and microtoroid array have been mentioned in chapter 2. Now, this only gap between separate experiment tools and complete experiment system is the container for microtoroid. Because mostly we will use microtoroid to detect some characteristic for liquid, it's important to construct a proper structure to meet the requirement. To solve this problem, we use a steel stage and coverslip to make a container called "micro-aquarium". Fig.12 shows the schematic diagram for that structure. The liquid will reach the steel stage through an infusion from a pump and then interact with the microtoroid. After that just assemble all elements into the system. The real experimental system can be seen in Fig.11.

Now we have our FLOWER system, but how does it work? Before we do the locking and detection procedure using the FLOWER system, it's important to find a resonance frequency with a high Q factor through the transmission spectrum to support our detection. Since without a resonance dip with high Q factor, it's difficult to finish the locking procedure, then it's hard to do the detection. Q factor in microtoroid can be viewed as a factor of how sensitive this microtoroid is. And it can be calculated through the following equation:

$$Q = \frac{\lambda_C}{\lambda_{FWHM}}$$

In this equation, λ_c means the center wavelength of that resonance dip on transmission spectrum, while λ_{FWHM} means the full-width half maximum of that resonance dip. Ideally, the Q factor of microtoroid can be as large as 10^{10}, which is much higher than other resonance systems. In real experiments, the acceptable Q factor for a microtoroid is about 10^6. For this step, we use oscilloscope in digilock software instead of the commercial oscillate scope, because it can give us less range of transmission spectrum, which means the output data for Q factor calculation is more accurate than the output data from oscillate scope. As I mentioned in the first chapter, the digilock device will import a continuous voltage ($\pm 6V, 100Hz$) to the laser source's voltage modulation. Since 1V voltage modulation will give the output wavelength a $20\mu m$ shift, what we can see through the digilock now is a transmission spectrum with a range of ± 120 μm to its center wavelength. If there's a narrow resonance dip in the transmission spectrum, we can add an attenuator at the voltage output to decrease the intensity of the voltage out by 10 times. Now the transmission spectrum has a range of ± 12 μm to its center wavelength. Export the spectrum data and calculate the Q factor by using the equation above. Repeat this step several times until we find a resonance dip that meets the requirements.

Once the proper resonance dip founded, then we can start the locking procedure. On the digilock software operation window, we can see a "Display" at the left side, which indicates the properties of the diagram shown in the window. To begin with locking, click "AutoLock" under the "Display" module, then right-click the diagram, choose "locking" and adjust the PID parameter above to keep the stability of locking. After that, the diagram of the transmission spectrum will be replaced

with a diagram with a sag of the line which indicates the locking. In this situation, the digilock will modulate the center frequency of laser beam output by giving a continuous voltage modulation so that the center frequency of the laser source fit with the resonance frequency. Not only does the voltage output goes to the laser source's voltage modulation, but it is also recorded to PC directly through a DAC card. The sampling frequency can up to 1000 Hz, which is better than other methods that use microtoroid for detection [12]. To test whether the locking is stable or not, a square wave will be produced from a function generator for testing. This square wave, which has frequency equals to 0.5 Hz and amplitude equals to 0.1V, will be induced to the laser source to modulate the center wavelength of the laser source. If we can see the same square wave through the monitor that tracks the voltage output from the digilock to modulate the center frequency of the laser source, it means the locking is successful and stable. After we make sure that this resonance dip can be locked successfully, we stop the locking procedure and infuse the liquid to the micro-aquarium by a pump. Then repeat the resonance dip finding step and locking step again, thus get the recorded voltage through the computer.

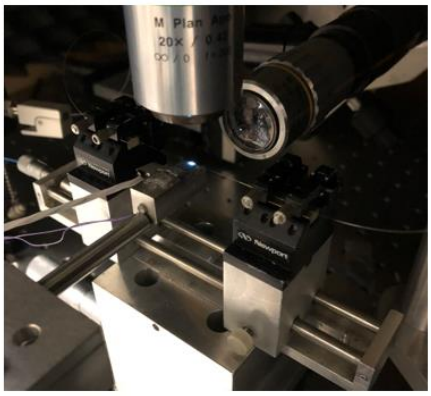

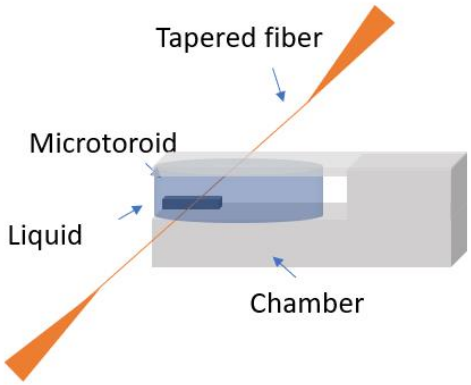

a) real setup b) schematic

Fig.10 Micro-aquarium for liquid infusion & detection

4. Thermal Effect in Microcavity

When we do the experiment about microtoroid, we figure out that no matter what the experiment setup keeps as well, there is still some blue shift when we do the liquid infusion. In the beginning, we just viewed it as the combined effect, but after we do the experiment for the control group with just buffer, we found the same phenomenon. So, this blue shift cannot be explained as particles combine to microtoroid, it can only be explained as environmental change. Since the environment material change from air to buffer is rapid, it's hard to explain the continuous resonance wavelength change in material change, the only parameter remained is the temperature. By reading the reference [13], it mentioned that there is a linear relationship between temperature and resonance frequency. So, the data without thermal effect can be founded by using the raw data to subtract the influence by thermal effect, then the final data is temperature-independent.

To figure out the relationship between resonance wavelength shift and temperature changes. We use a PID thermal controller to find its correlation. The temperature of the steel stage was heated up to 28 ℃ by using the PID thermal controller mounted on the stage. Then we turn off the heat up the program of the controller to cool down the whole stage while the resonance of the microtoroid was frequency locked in DI water. Now the wavelength shift with respect to time and the temperature decreases with respect to time can be recorded simultaneously by computer. From Fig. 12 (a) we can figure out that there's a first-order polynomial linear relationship between resonance wavelength shift and time. Fig. 12(b) shows there is also a linear relationship between temperature and time. Fig. 12(c) shows that the first order polynomial linear fit for the relationship between temperature and time, the r2 value of the linear fit was calculated 0.9995. Since the linear relationship shows up in both to the diagram, the relationship between resonance

wavelength shift and temperature should also be linear. Fig. 13(d) shows the result. The wavelength fit plotted out as a function of temperature. The linear relationship in the diagram is that with the temperature changes 1 ℃, the resonance wavelength will shift approximately 5 pm. We use this linear correlation to remove the thermal effect in data analysis about further experiments. Fig.14 shows up the schematic of the thermal effect related experimental setup.

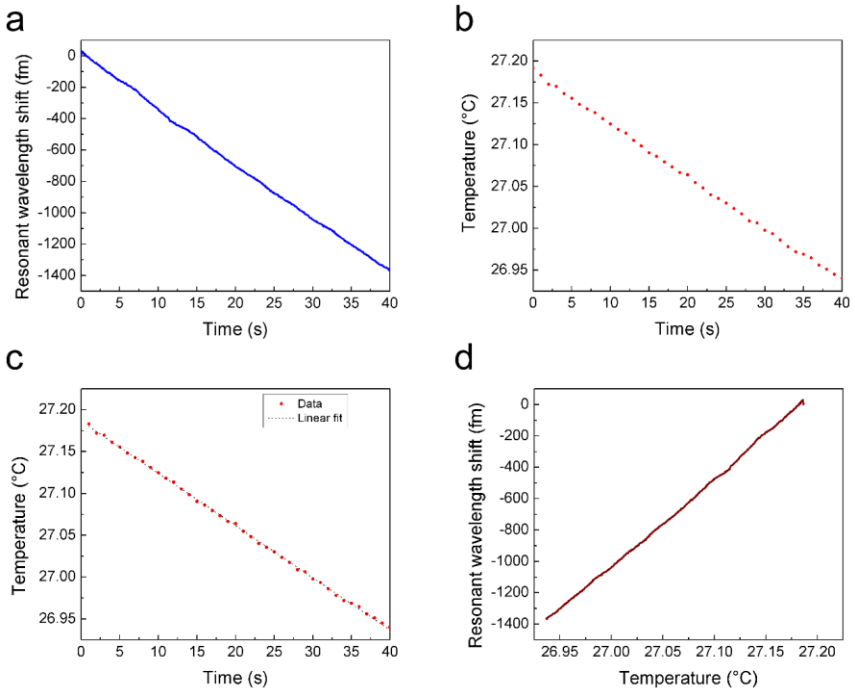

Fig.11 Relationship between temperature & WL shift

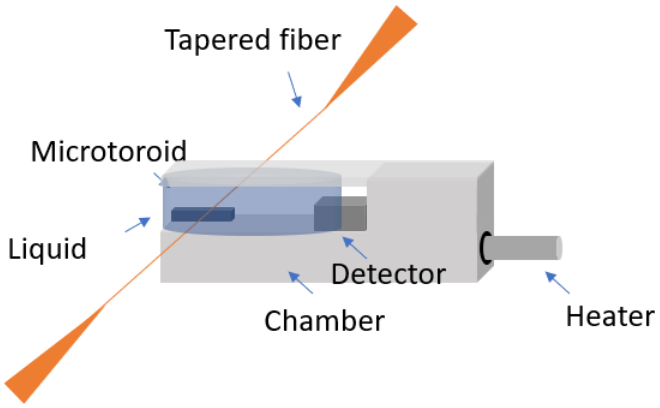

Fig.12 Thermal effect related experimental setup

5. Experiments about hCG detection

This chapter I will introduce the steps of doing experiments for hCG detection. After making the tapered fiber and microtoroid-production, the next step is to do the functionalization of microtoroid. In this step we will mount an antibody layer on microtoroid surface, thus giving it specialty for hCG detection. After the microtoroid functionalization, we will do the liquid preparation and infusion, data recording and analysis.

5.1 Microtoroid functionalization

After the microtoroid being made through laser reflowing and being certified that there's a high Q factor resonance wavelength from this resonator, we can do the functionalization step for the microtoroid. To combine the antibody on the microtoroid surface, it's impossible to combine it directly since it can not build up a chemical bond simply between silica surface and anti-hCG IgG antibody. So, at first, there should be a linker layer coated on the microtoroid surface as a bridge to maintain the antibody-microtoroid combination stable. To reach the goal, the silicon chip with microtoroid being Q-factor tested will be immersed in a custom synthesized silane-PEG-maleimide linker solution for 30 minutes to create the linker layer on microtoroid. After that, the silicon chips with microtoroids will be rinsed with DI (deionized) water to remove the linker remained on chips. Then the chip will be soaked in a 5 μg/ml solution of mouse monoclonal anti-hCG IgG antibody in PBS (Phosphate Buffered Saline). After that rinse, the chip with DI water again to remove the remained antibody on the silicon substrate. To prevent the functionalized microtoroid interact with air, the microtoroid will be immersed in 100 μg simulated human urine.

5.2 Liquid preparation and infusion

For this experiment, there are three types of liquid being utilized for the experiment: hCG diluted with different ratio from simulated urine, real samples from humans diluted with different ratio from simulated urine, hCG with different concentration diluted from PBS. The diluted rate for samples from human is from 10^2 dilutions to 10^6 dilutions and the concentration for hCG simulated sample is from 10 nM to 100aM. Not only the samples from human come from pregnant women in different stages, but it also comes from non-pregnant women and men as a control group. Simulated urine is a mixture of glycerine and sodium hydroxide and has the same pH as urine [14].

For liquid infusion, a peristaltic pump is used in our experiment as the infusion tool for the analyte with an operating rate of 10 $\mu l/s$. During the experiment, the liquid will be infused by the pump with an infusion needle attached to the steel stage of the micro-aquarium. The total volume for the micro-aquarium is about 100 μl. When doing experiments, the sequence of liquid infusion is from low concentration to high concentration. 100 μl of HCL and 200 μl of DI water will be used to rinse the steel chamber after the experiment.

5.3 Data recording

After all preparations above, using the Topica Digilock 110 frequency locking system to lock the laser frequency to the resonance frequency of microtoroid. This locking procedure was helped by a 2 kHz sinusoidal dither signal with 15 mV amplitude modulation. Now the range of the transmission spectrum we get through the computer is 300 fm. PID parameter for stable locking is 10, 100, 1 separately. Data was recorded through a 24-bit data acquisition card and outputted as a .tdms file by a LabView program for that DAC card.

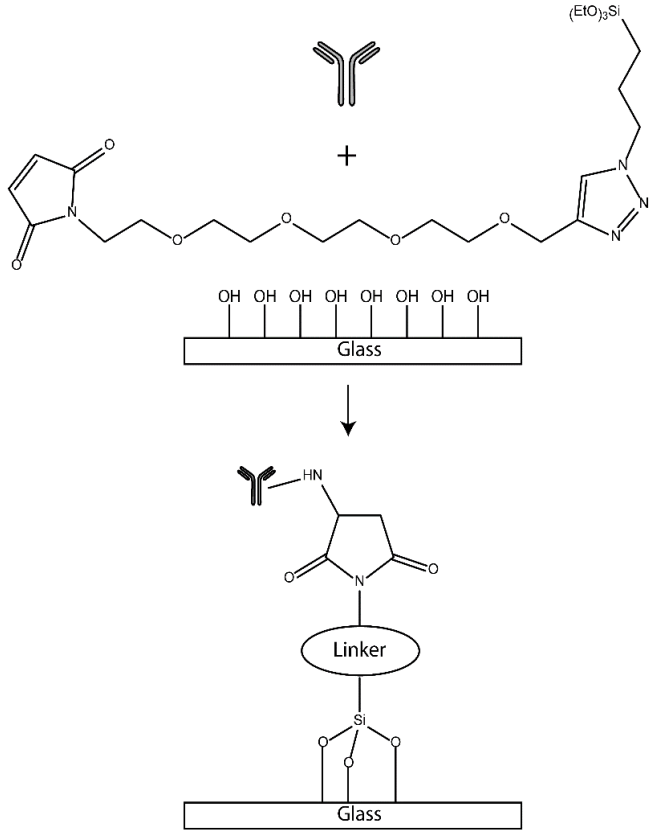

Fig.13 Schematic for surface chemical combination [18]

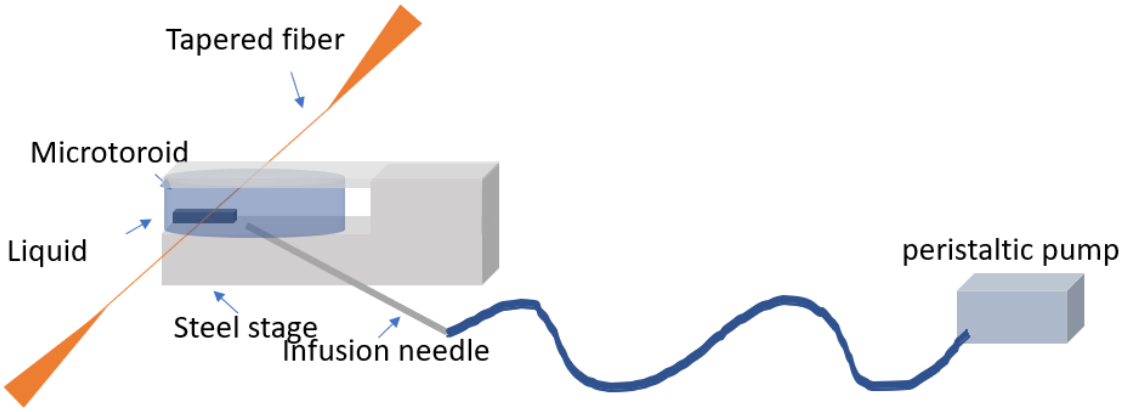

Fig.14 Schematic for infusion

6. Data Analysis

The recorded .tdms file will be analyzed through a MATLAB program. First, we import the data from the .tdms file to MATLAB and save the data to several matrices. Because there is a relationship between recorded modulation voltage and output center wavelength shift, so we can plot out a diagram to imply the resonance wavelength shift with respect to time. Fig.16 (a) shows that diagram of background noise measurement. This diagram contains the resonance wavelength shift in 20 seconds. There is also a polynomial fit to subtract the thermal effect during the experiment. After that, we use the Fourier transform to convert the information from spatial domain to frequency domain. Then the periodic noise can be viewed from the frequency domain diagram as a peak. These peak frequencies can be filtered by using a custom-built script. The frequencies higher than 1000 Hz are also been filtered. The diagram after Fourier transform can be seen on Fig.16 (b) and the frequency spectrum after filtering can be seen on Fig.16 (c). Last, we do the inverse Fourier transform for that filtered data. A median filter of 1000 points was also applied for this data for data smoothing. Fig16. (d) shows the result after Fourier filtering and inverse Fourier transform, the red line in the diagram shows the result after the median filter. The background noise level is measured as 0.0217 +/- 0.0069 fm at 1 s, and 0.0002 +/- 0.0001 fm at 1 ms after Fourier & median filtering. Since the thermal shift has been tested as a 1 order polynomial, it was removed by subtracting a straight line corresponding to the initial slope of the filtered signal.

After the data filtered by the Matlab program, the Origin software was used to do the polynomial fit and result diagram plot out.

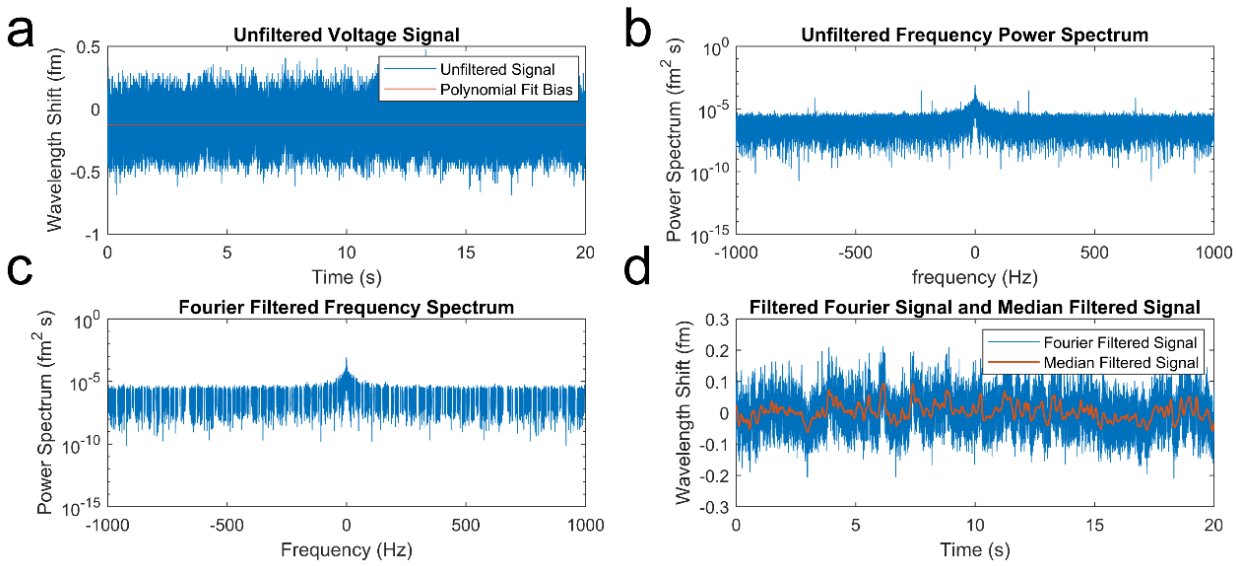

Fig.15 Data analysis through Matlab

7. Results

Based on the experiments, we first used the hCG diluted from simulated urine for detection to explore the sensitivity of our FLOWER system for hCG. The solution concentration ranging is from 100 aM to 10 nM over the toroid's surface. The same microtoroid was used in this experiment to keep the same experiment variable.

Fig.16 (a) shows the resonance wavelength shifts with respect to time in different concentration when we use the functionalized microtoroid for detection. From the recorded data, the FLOWER system can detect hCG over 6 order of magnitude concentration range. The limitation of detection was calculated to be 120 aM by using the three-sigma method, which equals to three times of standard deviation of repeated blank infusion experiments. The lowest experimentally detected concentration we measured in our experiments was 1 fM. Fig.16 (b) shows the curve of resonance wavelength shift slope and hCG concentration. Data utilized in this diagram comes from the average and standard deviation of three independent experiments.

Fig.16 (c) shows the control group result that uses the bare microtoroid without functionalization for detection. In this situation, the first obviously detected resonance wavelength shift was at the concentration of 10 fM. Without the coated antibody layer, what we actually detected is the physisorption of hCG. The isoelectric point of urine hCG is below 7 [15], therefore, it has negative charges at pH 7.4 and is capable of forming a monolayer on silica surface [16]. Fig.16 (d) shows the curve of resonance wavelength shift slope and hCG concentration. We figure out the sensitivity is worse than the toroid with functionalization because there is no antibody on the microtoroid for specificity binding. Data utilized in this

diagram comes from the average and standard deviation of two independent experiments.

Due to the result from functionalized microtoroid and unfunctionalized microtoroid, the dynamic range and sensitivity increased a lot after functionalization with anti-hCG. This can be explained by the increased affinity of the microtoroid to hCG after functionalization. This increased affinity corresponds to a slower unbinding rate and may also partially suppress the inhibition caused by the accumulation of negative charges on the silica microtoroid's surface.

Fig.17 shows the result of real human urine samples. Fig.17 (a)-(c) shows the experiment result of hCG detection from the urine of pregnant women during the 1^{st}, 2^{nd}, 3^{rd} trimesters of pregnancy, respectively. Three different dilutions for each sample were tested using the same microtoroid via FLOWER system. The amounts of hCG in the 10^6 times diluted samples are estimated to be 37 fM, 3 fM, and 11 fM at each trimester. Based on the experiment result, the lowest hCG concentration we detected for real urine sample is 3 fM.

Fig.17 (d) shows the comparison between the measurement result from the hCG test strip and the result from FLOWER system. The concentration measurement of the real human sample comes from the resonance wavelength shift & concentration relationship in simulated urine with hCG. The real sample FLOWER system testing result agrees with the result of the hCG test strip.

Fig.17 (e)-(f) shows the control group result. We use the urine sample from man and non-pregnant women for the control group experiment. From the resulting plot, we can not figure out any resonance wavelength shift when sample is diluted 10^6 times and 10^4 times, which agree with the result from simulated urine result

since the concentration of hCG in men or non-pregnant women urine is about 120-150 fM [17].

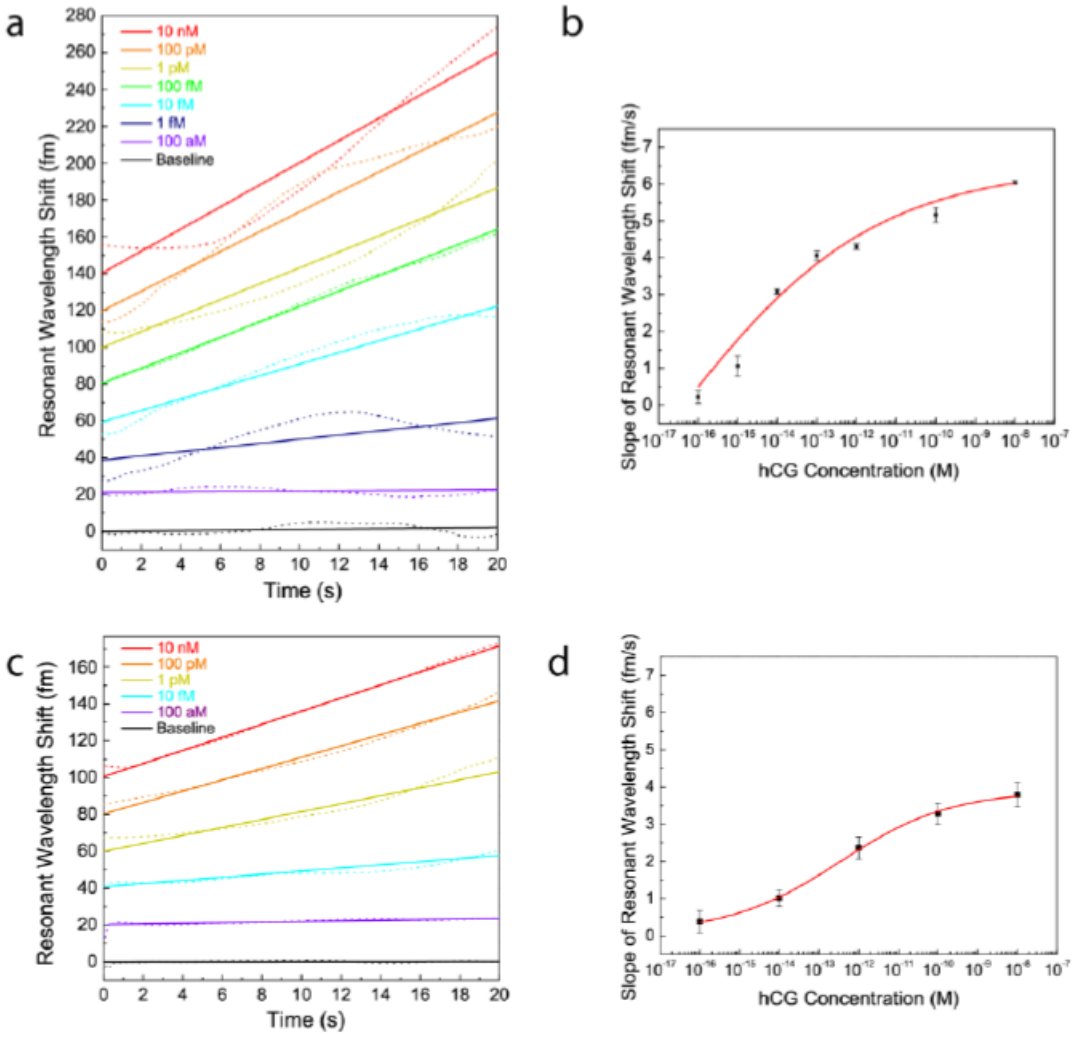

Fig.16 Result of hCG detection from a simulated sample

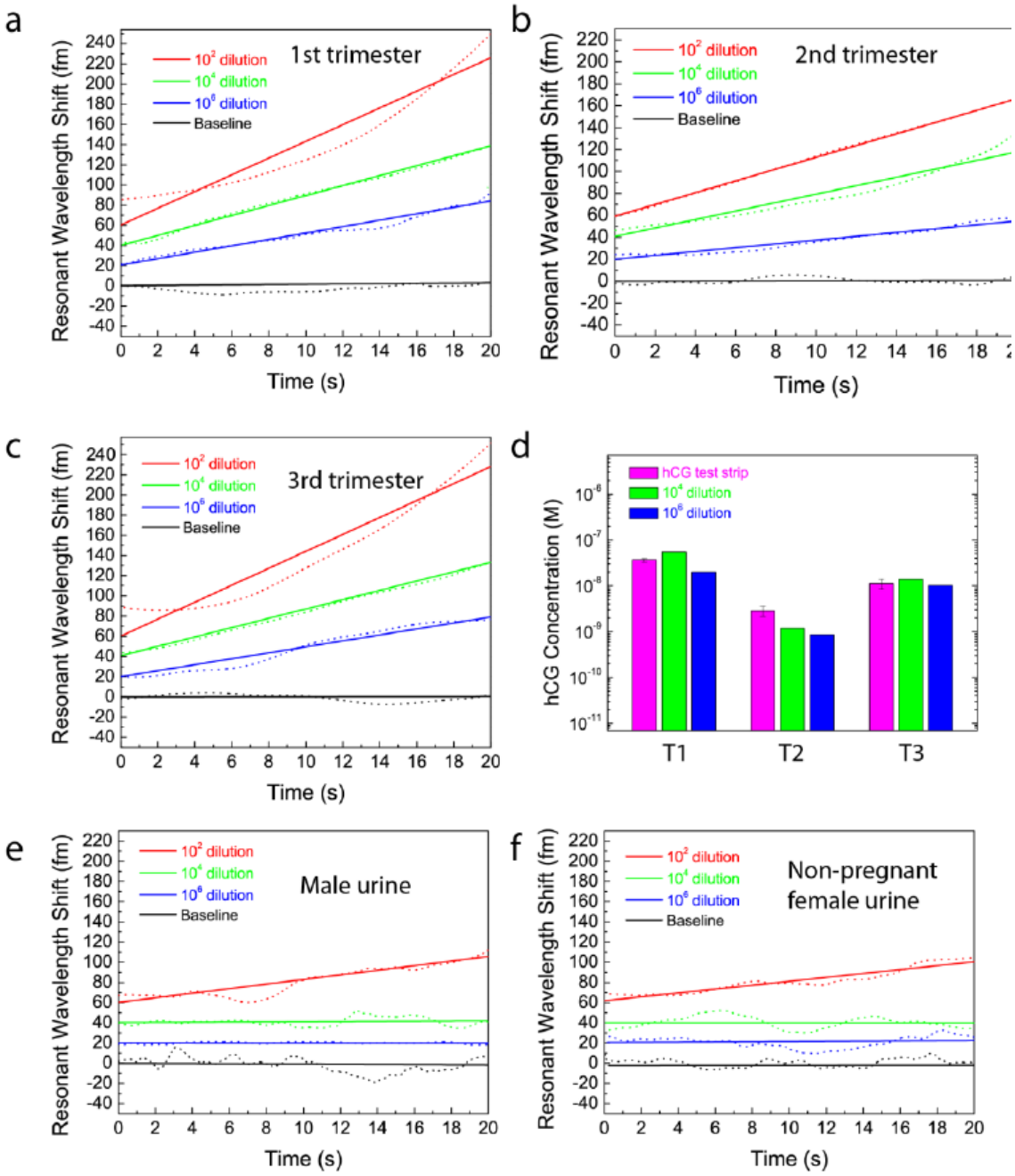

Fig.17 Result of hCG detection from real sample

8. Summary

From the result above, we have demonstrated the detection of the lowest hCG concentration in simulated urine is 1fM, while the lowest hCG concentration being measured in the real urine sample is about 3 fM. Our approach can provide high SNR measurement over a large dynamic range. Figure.18 shows the outstanding performance of hCG compared with other methods for hCG detection. Not only does the FLOWER system has greater dynamic range and sensitivity, but it also has less requirement like target molecule binding or fluorescence binding, which makes detection easier than these old methods. Moreover, its real-time characteristic also helps us to get the result faster than other methods.

In conclusion, we have demonstrated a label-free method which has the potential to detect the hCG in extremely low concentrations, which may be used in doping measurement.

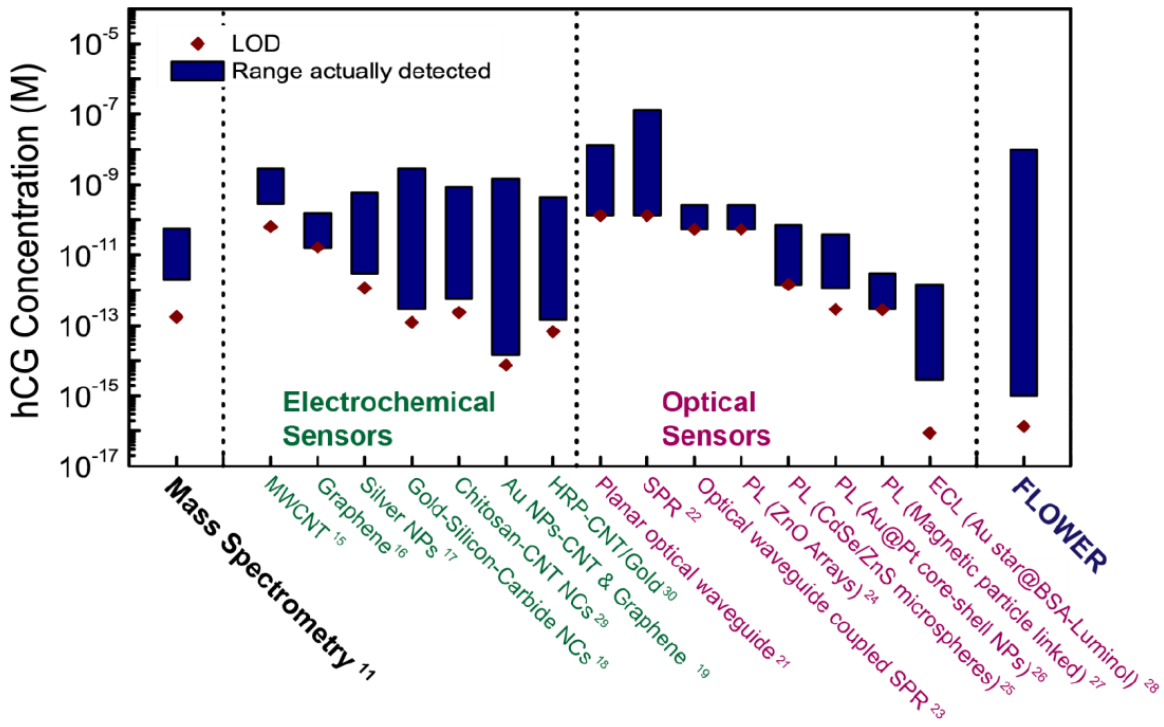

Fig.18 comparison of FLOWER and other sensing methods

9. Reference

1. Lidgate, S. C. M. , P. Sewell , and T. M. Benson . "Conformal mapping: Limitations for waveguide bend analysis." IEE Digest 149.5(2002):262-0.
2. Oxborrow, Mark . "How to simulate the whispering-gallery modes of dielectric microresonators in FEMLAB/COMSOL." Laser Resonators & Beam Control IX International Society for Optics and Photonics, 2007.
3. Zhang, Xiaomin , and A. M. Armani . "Silica microtoroid resonator sensor with monolithically integrated waveguides." *Optics Express* 21.20(2013):23592.
4. Biggs, Bradley W. , H. K. Hunt , and A. M. Armani . "Selective patterning of Si-based biosensor surfaces using isotropic silicon etchants." *Journal of Colloid & Interface Science*369.1(2012):477-481.
5. Lin, H B , et al. "Excitation localization principle for spherical microcavities. " *Optics Letters* 23.24(1998):1921-3.
6. Braginsky, V. B. , M. L. Gorodetsky , and V. S. Ilchenko . "Quality-factor and nonlinear properties of optical whispering-gallery modes." *Physics Letters A* 137.7-8(1989):393-397.
7. Klitzing, W. Von , et al. "Very low threshold lasing in Er3+ doped ZBLAN microsphere." *Electronics Letters*35.20(1999):1745-1746.
8. Cai, Ming , and K. Vahala . "Highly efficient hybrid fiber taper coupled microsphere laser." *Conference on Lasers & Electro-optics* IEEE, 2001.
9. Baer, T. . "Continuous-wave laser oscillation in a Nd:YAG sphere." *Optics Letters* 12.6(1987):392-394.
10. Knight, J. C , et al. "Phase-matched excitationof whispering-gallery-mode resonances by a fibertaper." *Optics Letters*22.15(1997):1129-1131.

11. Armani, D. K. , et al. "Ultra-high-Q toroid microcavity on a chip." *Nature* 421.6926(2003):925-928.
12. Su, Judith , A. F. Goldberg , and B. M. Stoltz . "Label-free detection of single nanoparticles and biological molecules using microtoroid optical resonators." *Light: Science & Applications* 5.1(2016):e16001.
13. Strekalov, D. V. , et al. "Temperature measurement and stabilization in a birefringent whispering gallery mode resonator." *Optics Express* 19.15(2011):14495-501.
14. Hamorsky, Krystal Teasley , et al. "A PROTEIN SWITCH SENSING SYSTEM FOR THE QUANTIFICATION OF SULFATE." *Analytical Biochemistry* 421.1(2012):172-180.
15. Sutton, Jaime M. . "Charge variants in serum and urine hCG." *Clinica Chimica Acta* 341.1-2(2004):0-203.
16. J Dostálek, et al. "Surface plasmon resonance biosensor based on integrated optical waveguide." *Sensors and Actuators B (Chemical)* 76.1-3(2001):8-12.
17. Stenman, U. H. , et al. "Serum levels of human chorionic gonadotropin in nonpregnant women and men are modulated by gonadotropin-releasing hormone and sex steroids." *Journal of Clinical Endocrinology & Metabolism* 64.4(1987):730-6.
18. Su, Judith , A. F. Goldberg , and B. M. Stoltz . "Label-free detection of single nanoparticles and biological molecules using microtoroid optical resonators." *Light: Science & Applications* 5.1(2016):e16001.